Synchronization in the van der Pol-Duffing system via elastic and dissipative couplings

U. Uriostegui-Legorreta[a] and E. S. Tututi[b,*]

[a]*CINVESTAV-IPN, Unidad Guadalajara,*
Av. del Bosque 1145, Col. el Bajío, Zapopan Jalisco, 45019, México.
[b]*Facultad de Ciencias Físico Matemáticas, UMSNH,*
Av. Francisco J. Mújica S/N, Morelia Michoacán, 58060, México.
*e-mail: ulises.fismat@gmail.com, eduardo.tututi@umich.mx

The classical master-slave configuration allows synchronizing pairs of unidirectionally coupled systems in a relatively simple manner. However, it has been found that this scheme has a limitation: for certain systems including those with chaotic dynamics, the scheme fails at inducing synchronization. In this work a modified master-slave scheme, based on the combination of elastic and dissipative couplings, is presented. We focus on a possible solution for this limitation by illustrating our method through the van der Pol and Duffing oscillators and analyzing three different ways of coupling. We obtain, synchronization in both oscillators.

Keywords: Nonlinear dynamics; control of chaos; synchronization.

1. Introduction

Due to numerous works on chaos in recent years, current research on this topic comprises chaotic systems in diverse areas such as lasers, chemical reactions, electronic circuits, biological systems, among others. The work of Pecora and Carroll on synchronization [1] and experiments with circuits operating in a chaotic regime give a great impulse to the study of chaotic systems. Particularly, low-dimensionality systems have been of interest in order to understand the synchronization and chaotic behavior in nature. The most studied and representative systems are the Lorenz, Chua, Rössler, van der Pol and Duffing ones [2–7].

The van der Pol and Duffing oscillators are the paradigmatic circuits to study chaos in systems of low-dimensionality. These systems give rise to limit cycles and prototypes of strange attractors. Studies focused on the van der Pol oscillator reveal that the system possess an interesting dynamical structure when the oscillator is under an external forcing. In fact, the system exhibits complex bifurcation structures with an important number of periodic states, a chaotic region and islands of periodic states, showing, in addition, transitions from chaos to stable states [8]. On the other hand, the Duffing oscillator presents damping oscillations when the system is autonomous. In the presence of an external harmonic forcing, the system leads to hysteresis, multistability, period-doubling, and intermittent scenarios of chaos. In addition, we can mention that two coupled van der Pol oscillators give a rich fractal structure. Moreover, other systems based on this oscillator, such as identical oscillators, have also been analyzed. The dynamics based on identical or distinct linear oscillators presenting the same kind of attractors is still under study [8]. The dynamics of these systems in

states of different attractors is of current interest and it could originate important information. A model of coupled oscillators, each being in its own attractor regime, could be useful to represent hysteresis or resonant phenomena founded in biological or electromechanical systems [9]. Some applications of the van der Pol and Duffing oscillators go from physics to biology, electronics, chemistry and many other fields. For instance, a possible application of synchronization in chaotic signals, is for implementing secure communication systems, since chaotic signals are usually broadband, noise-like, and difficult to predict their behavior [10–12]. In robotics, the oscillators have been included to control hip joints and knees of human-like robots to synchronizing the mechanical system, giving approximate paths to the robot legs. The signals generated can also be used as trajectories of reference for the feedback control [13, 14]. Other applications are in artificial intelligence. In fact, the oscillators show usefulness to training neuronal network and recognition of chaotic systems [15, 16].

The synchronization is observed in several natural and technical systems, going from cardiac cells to coupled lasers [17, 18]. Thus, the comprehension of mutual interactions between coupled oscillators and their synchronization results an important issue. As far as the coupling between the van der Pol and Duffing oscillators is concerned, we can mention three different couplings, namely: gyroscopic, dissipative and elastic [19–24]. Among the diverse way of coupling, the most used are the elastic and dissipative ones [25,26]. In a previous work [24], it is analyzed a different approach of synchronizing two distinct oscillators of low-dimensionality, by using the aforementioned couplings. In this work, we study and compare three types of couplings by using the van der

Pol-Duffing system; the elastic, the dissipative and the used previously by Uriostegui *et al.* [24], in order to achieve synchronization in a master-slave system. It is important to remark that the studies in the literature on this kind of synchronization is based only on one coupling.

An outline of this work is as follows. In Sec. 2, it is briefly studied the main features of the van der Pol and Duffing oscillators. In Sec. 3, we study and compare three types of couplings using the van der Pol-Duffing system in the master-slave configuration to achieve synchronization. In Sec. 4, the final remarks and an outlook are presented.

2. Dynamics of the systems

As a dynamical system, the van der Pol oscillator is one with nonlinear damping. The evolution is governed by

$$\ddot{x} - \mu(1 - x^2)\dot{x} + x = A_2 \cos(\omega_2 t), \tag{1}$$

where, as usual, the x variable denotes the position, t the time, and μ is a parameter that governs the nonlinearity and damping of the system. The external forcing is given by the harmonic function, with amplitude A_2 and frequency ω_2. In order to identify the potential, we cast Eq. (1) as

$$\ddot{x} - \mu(1 - x^2)\dot{x} + \frac{\partial U_2(x)}{\partial x} = A_2 \cos(\omega_2 t), \tag{2}$$

where we have defined the function

$$U_2(x) = \frac{1}{2}x^2, \tag{3}$$

as the energy potential of the van der Pol oscillator, which represents a simple well (see Fig. 1a)). The potential has a minimum located at $x = 0$. In order to express Eq. (1) as a dynamical system and to analyze the fixed points, we set $\dot{x} = u$ and drop the forcing to obtain

$$\dot{x} = u,$$
$$\dot{u} = \mu(1 - x^2)u - x. \tag{4}$$

As it is well known, for a dynamical system with n degrees of freedom, $\dot{\mathbf{x}} = \mathbf{f}(\mathbf{x})$, the fixed points, $\mathbf{x}^* = (x_1^*, x_2^*, \ldots x_n^*)$, are determined by the relation $\dot{\mathbf{x}} = \mathbf{f}(\mathbf{x}^*) = 0$. In the case of Eq. (4) the only fixed point is located at $(x^* = 0, u^* = 0)$. For the $A_2 = 0$ case, the van der Pol system satisfies the Liénard theorem, giving a limit cycle around the origin in the phase space [25].

On the other hand, the Duffing oscillator is a nonlinear dynamical system governed by

$$\ddot{y} + \alpha\dot{y} - y + \varepsilon y^3 = A_1 \cos(\omega_1 t), \tag{5}$$

where α is the damping parameter, ε is a positive constant that controls the nonlinearity of the system, A_1 and ω_1 are the amplitude and frequency, respectively, of the external forcing. As before, we can identify a potential $U_1(y)$ in the Duffing system given by

$$U_1(y) = -\frac{1}{2}y^2 + \frac{1}{4}\varepsilon y^4. \tag{6}$$

The potential represents a double well shown in Fig. 1b). The local minima of this potential are located in $y = \pm 1/\sqrt{\varepsilon}$ and the local maximum is located at $y = 0$. As a dynamical system the Duffing equation in Eq. (5) (no forcing) can be written as
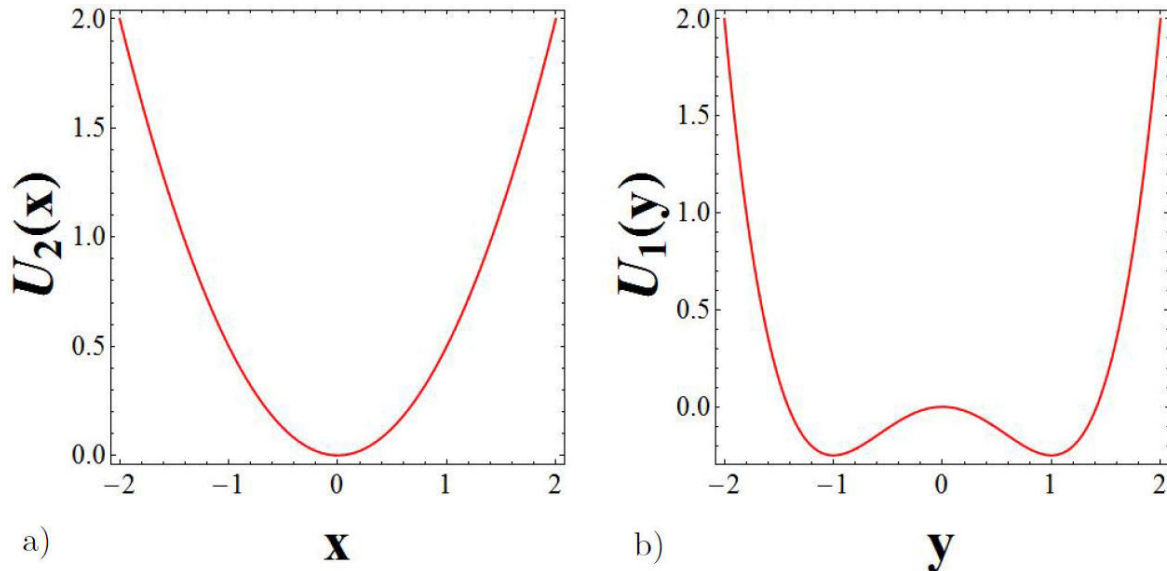

FIGURE 1. The potentials $U_2(x)$ and $U_1(y)$. a) The potential corresponds to the van der Pol oscillator. b) The Duffing oscillator ($\varepsilon = 1$).

$$\dot{y} = v,$$

$$\dot{v} = -\alpha v + y - \varepsilon y^3. \tag{7}$$

The fixed points for this system are located in the phase space at $(0,0)$ and $(\pm 1/\sqrt{\varepsilon}, 0)$. The $(0,0)$ is a saddle point, while the others, depending on the parameter α, the points can be stable or unstable. For the $\alpha > 0$ case the points result stables. For $\alpha = 0$, the resulting dynamics is of type center and finally, for $\alpha < 0$ case, the points result unstable. In particular, when the damping is positive ($\alpha > 0$), the trajectory of the system is a spiral stable, conversely, when the damping is negative ($\alpha < 0$), the trajectory is a spiral unstable at the fixed points $(\pm 1/\sqrt{\varepsilon}, 0)$ in both cases.

3. Master-slave synchronization in the van der Pol-Duffing system

In this section, three different couplings for the van der Pol-Duffing system are studied and compared among themselves, namely: the elastic, the dissipative and the one that combines an elastic and dissipative couplings employed by Uriostegui *et al.,* [24]. Let us stress that most of the research on synchronization is based on autonomous systems of three dimensional or higher [27–29]. It is important to mention that the synchronization between coupled forced systems of low-dimensionality has been hardly studied [30, 31] since there are few low-dimension chaotic systems with forcing known in the literature. Three of the most studied nonautonomous systems of low-dimensionality with forcing are the Duffing, van der Pol, and Rayleigh, since much of the dynamical features embedded in the physical systems can be realized on these systems [32–34]. One important implication is that a two dimensional continuous dynamical system cannot give rise to strange attractors. In particular, chaotic behavior arises only in continuous dynamical systems of three dimensions or higher. Most of the research on synchronization is based on autonomous systems that satisfy the Poincaré-Bendixson theorem.

The dynamics of the oscillators under study is described by Eqs. (1) and (5). The values of the parameters we use to carry out the numerical study are as follows: $\mu = 0.8$, $\alpha = 0.25$, $\varepsilon = 1$, $A_1 = 0.3$, $\omega_1 = 1$, $A_2 = 1$ and $\omega_2 = 0.4$. In Fig. 2 it is displayed the respective trajectories with the initial conditions $x(0) = 0.8$, $y(0) = 2.0$, $u(0) = 1$ and $v(0) = -1$. In addition, we would like to mention that the differential equations are numerically solved by using the Runge-Kutta method of fourth order.

In the configuration master-slave, the Duffing oscillator acts as master and the van der Pol oscillator as slave. For this case we have

$$\text{Master}: \begin{cases} \dot{y} = v, \\ \dot{v} = -\alpha v + y - \varepsilon y^3 + A_1 \cos(\omega_1 t), \end{cases} \tag{8}$$

$$\text{Slave}: \begin{cases} \dot{x} = u, \\ \dot{u} = \mu(1-x^2)u - x + A_2 \cos(\omega_2 t) + K(y - x). \end{cases} \tag{9}$$

In this instance, the coupling corresponds to an elastic one and it is represented by $K(y - x)$, being K a coupling parameter to be varied. For the $K = 0$ case, the system decouples. The coupling is a lineal feedback to the slave oscillator and it can be seen as a perturbation for each oscillator in the system, proportional to the difference of the position, what is called in literature an elastic coupling. We are interested in to study how the dynamics of the system evolves as the constant coupling K changes.
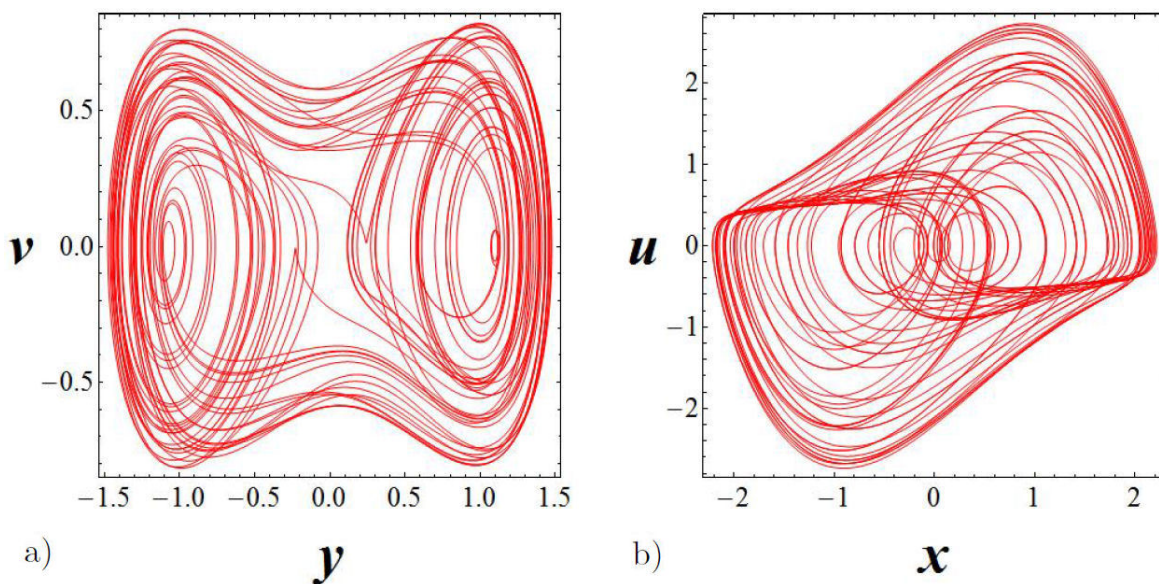

FIGURE 2. a) Duffing oscillator. b) van der Pol oscillator.

In particular, let us consider the $K \gg \mu$ case. Hence, the Eq. (9) can be approximated as

$$\ddot{x} + (1 + K)x \approx A_2 \cos(\omega_2 t) + Ky, \qquad (10)$$

which represents a simple harmonic oscillator with an external forcing. The solutions to the equation are harmonic functions, whose amplitudes can be as large as the corresponding to the particular solution provided by the forcing, particularly by the term Ky due to the master oscillator. This implies that total synchronization could not be possible for values of K large enough.

In general, the synchronization problem reduces to finding a suitable value of the coupling strength K, (denoted as K^*) being in the range $K \geq K^* > 0$, such that the master and slave systems synchronize. Thus, for a coupling strength K^*, when the synchronization is reached, the error function goes to zero:

$$\lim_{t \to \infty} | y(t) - x(t) | = \lim_{t \to \infty} | v(t) - u(t) | = 0. \qquad (11)$$

When the system is partially synchronized, for a certain value of K^*, the error functions satisfy

$$\lim_{t \to \infty} | y(t) - x(t) | \leq \delta, \qquad (12)$$

$$\lim_{t \to \infty} | v(t) - u(t) | \leq \tau, \qquad (13)$$

for given positive values $\delta, \tau > 0$. In some cases, it can be reached total synchronization in only one channel while in the other, it can be only obtained partial or null synchronization.

The bifurcation diagrams are achieved by means of the error functions $| y(t) - x(t) |$ and $| v(t) - u(t) |$ by taking K as a control parameter to be varied in small steps, from 0 to 200. As it is well known, the way of corroborating whether two coupled systems are synchronized or not is through the error functions, they must go to zero as the time goes to infinity. For our case, the bifurcation diagrams of the error functions $| y(t) - x(t) |$ and $| v(t) - u(t) |$, allow us to find the range of values for K in which the synchronization is reached in the

channels $y - x$ and $v - u$ (see Figs. 3a) and b)). As it is observed, there is not synchronization in this kind of coupling, since the error functions for the channels $y - x$ and $v - u$ do not vanish. This can be explained in terms of Eq. (10). In order to see this, let us observe that the errors $e_1 = y - x$ and $e_2 = v - u$ can be calculated from Eqs. (8) and (9) as:

$$\dot{e}_1 = \dot{y} - \dot{x} = e_2,$$
$$\dot{e}_2 = -\alpha v + y - \varepsilon y^3 + A_1 \cos(\omega_1 t)$$
$$\quad - \mu(1 - x^2)u + x - A_2 \cos(\omega_2 t) - K(e_1). \qquad (14)$$

whose behavior is displayed in Fig. 3 as a function of t, for a value of $K = 200$.

In order to numerically corroborate that there is not synchronization in any of the channels under study, let us analyze the phase space in the $y - x$ and $v - u$ channels for a particular value $K = 200$. For which, the master system (Duffing oscillator) is working in the chaotic regime and the dynamics of the van der Pol oscillator is not being controlled by Duffing oscillator as it can be observed from Figs. 5c) and d). If we had have synchronization we could observe a straight line at $45°$ on both channels, but it is not the case.

Let us now discuss the synchronization when the oscillators are interacting through a dissipative coupling, represented by

$$\text{Master}: \begin{cases} \dot{y} = v, \\ \dot{v} = -\alpha v + y - \varepsilon y^3 + A_1 \cos(\omega_1 t), \end{cases} \qquad (15)$$

$$\text{Slave}: \begin{cases} \dot{x} = u, \\ \dot{u} = \mu(1 - x^2)u - x + A_2 \cos(\omega_2 t) + H(v - u). \end{cases} \qquad (16)$$

where $H(v - u)$ represents the dissipative coupling, being H used as a parameter. As before, for the case in which $H = 0$, the oscillators become to be decoupled. Similar to the elastic coupling, the term, $H(v - u)$, used in this case, is a lineal feedback to the slave oscillator. Physically, the dissipative coupling $H(v - u)$ drives the two interacting systems to a
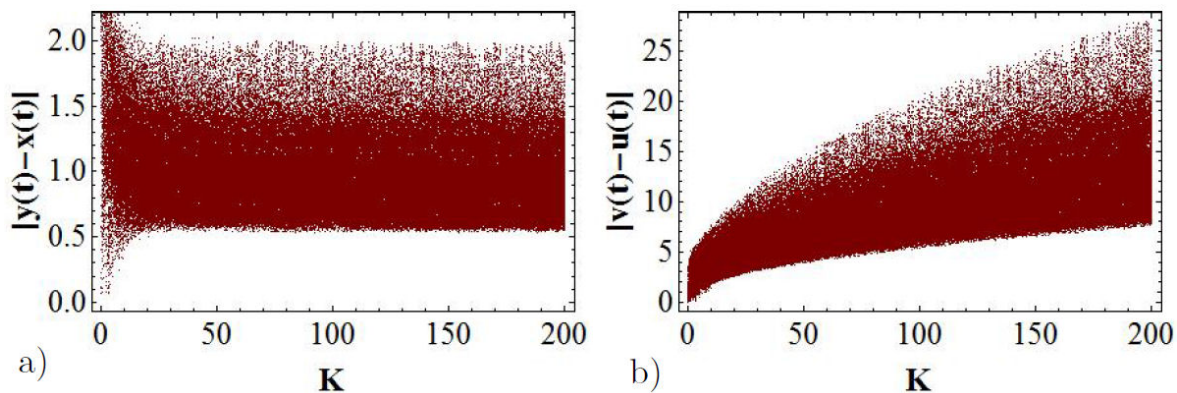

FIGURE 3. Bifurcation diagrams for the error functions: in (a) it is represented $| y(t) - x(t) |$, and in (b) $| v(t) - u(t) |$, both as a function of the parameter K.
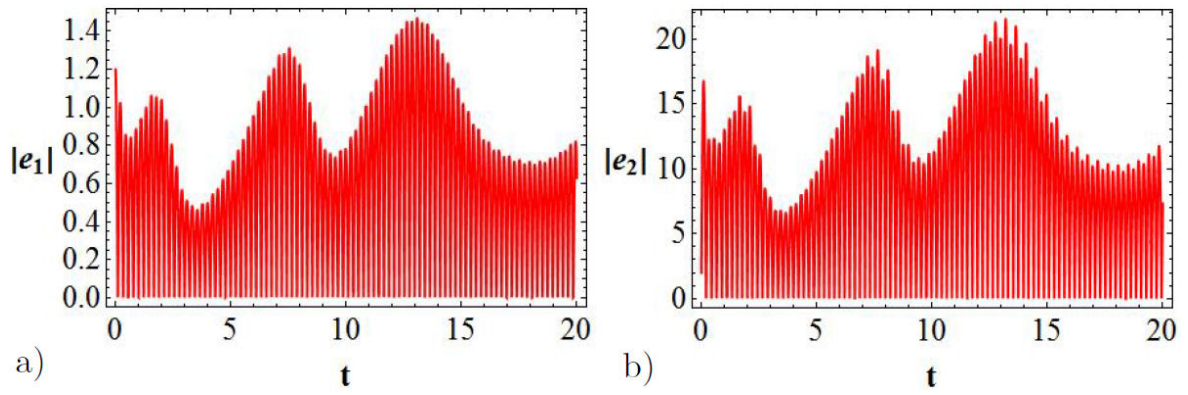
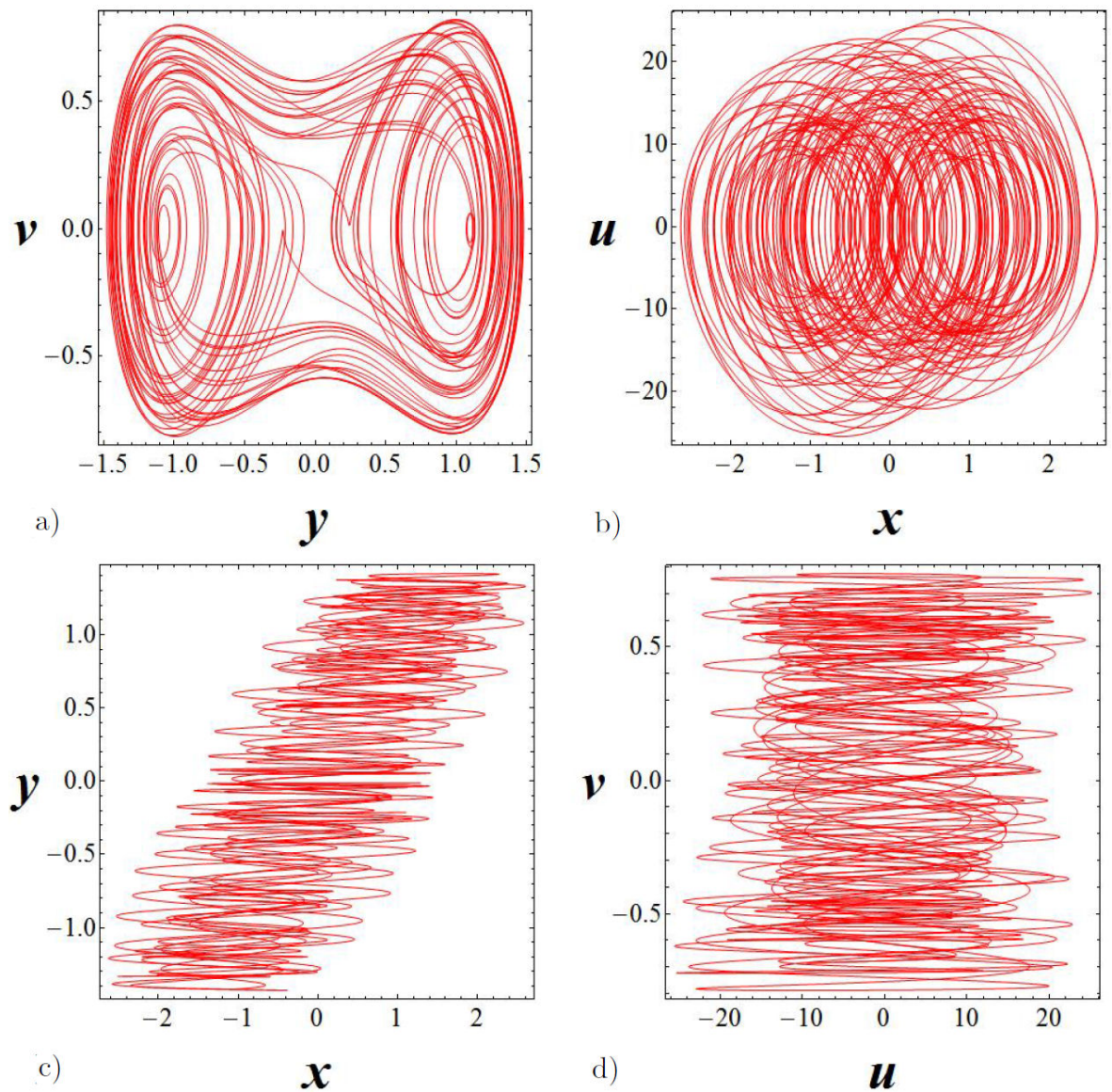FIGURE 4. Error functions $|e_1|$ and $|e_2|$ as a function of t, for a value $K = 200$.

FIGURE 5. Elastic coupling, for a parameter control of $K = 200$. In a) the Duffing oscillator. In b) the van der Pol oscillator. In c) and d) the phase space for the $y - x$ and $v - u$ channels.
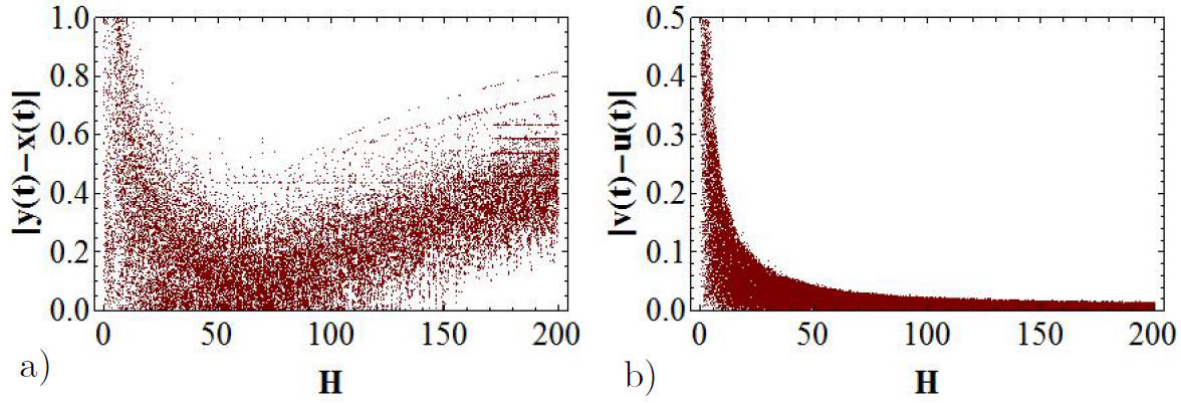
FIGURE 6. Bifurcation diagrams for the error functions: In a) it is displayed $\mid y(t) - x(t) \mid$, and in b) $\mid v(t) - u(t) \mid$, both as a function of the parameter H.
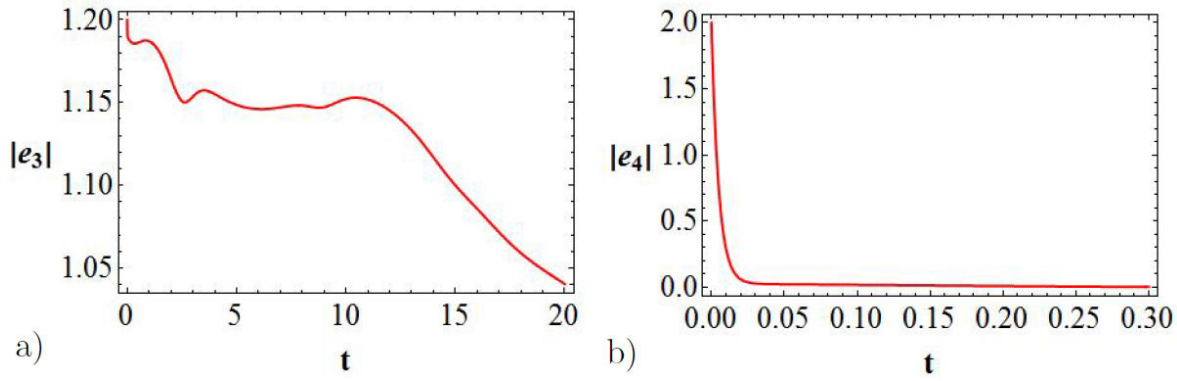

FIGURE 7. Error functions $|e_3|$ and $|e_4|$, for $H = 200$.

more homogeneous regime where their states coincide. As a result, this coupling directly favors synchronization of the oscillators. In order to get more insight in the solution, let us consider the case of H large enough such that $H \gg \mu$. Thus, we can neglect the nonlinear contribution in Eq. (16) to obtain

$$\ddot{x} + H\dot{x} + x \approx A_2 \cos(\omega_2 t) + H\dot{y}.$$

This equation represents a damped harmonic oscillator with forcing, where the term $H\dot{y}$, is due to the master oscillator. Clearly, for large t, the transient solution can be neglected and the behavior of the slave oscillator is dominated by the particular solution, that is to say by the master oscillator.

We study the evolution of the system by varying the H parameter. The bifurcation diagrams are obtained by means of the error functions $\mid y(t) - x(t) \mid$ and $\mid v(t) - u(t) \mid$, with H varied from 0 to 200 in small steps. These diagrams enable us to find the range of values for H in which the synchronization could be reached as it is shown in Figs. 6a) and b). Notice that in the $y - x$ channel no synchronization exists, since the error function $\mid y(t) - x(t) \mid$ results too large. For the $v - u$ channel, the synchronization could be reached for rather large values of H. For the dissipative coupling, the errors $e_3 = y - x$ and $e_4 = v - u$, are determined by subtracting

Eqs. (15) and (16), given

$$\dot{e}_3 = \dot{y} - \dot{x} = e_4,$$

$$\dot{e}_4 = -\alpha v + y - \varepsilon y^3 + A_1 \cos(\omega_1 t)$$
$$- \mu(1 - x^2)u + x - A_2 \cos(\omega_2 t) - H(\dot{e}_3). \quad (17)$$

The behavior of these functions is shown in Fig. 7 for a value of $H = 200$.

Let us analyze the space phase for the $y - x$ and $v - u$ channels for a specific value of $H = 200$. In this case, the Duffing oscillator is in a chaotic regime. In Fig. 8c) we can appreciate the fact that in the $y - x$ channel there is no synchronization, while in $v - u$ channel there is total synchronization (Fig. 8d)).

For certain systems, it is not possible to reach synchronization when the classical master-slave scheme is used. Specifically, there are cases where it is impossible to find a coupling constant K such that the systems reach synchronization, as it occurs for the systems described by Eqs. (8) and (9). In some cases, the systems reach partial or total synchronization in only one channel as it occurs for the dynamics contained in Eqs. (15) and (16), depending of the value H. Variations to the master-slave scheme for some systems have been proposed to solve certain kind of problems [35–38].
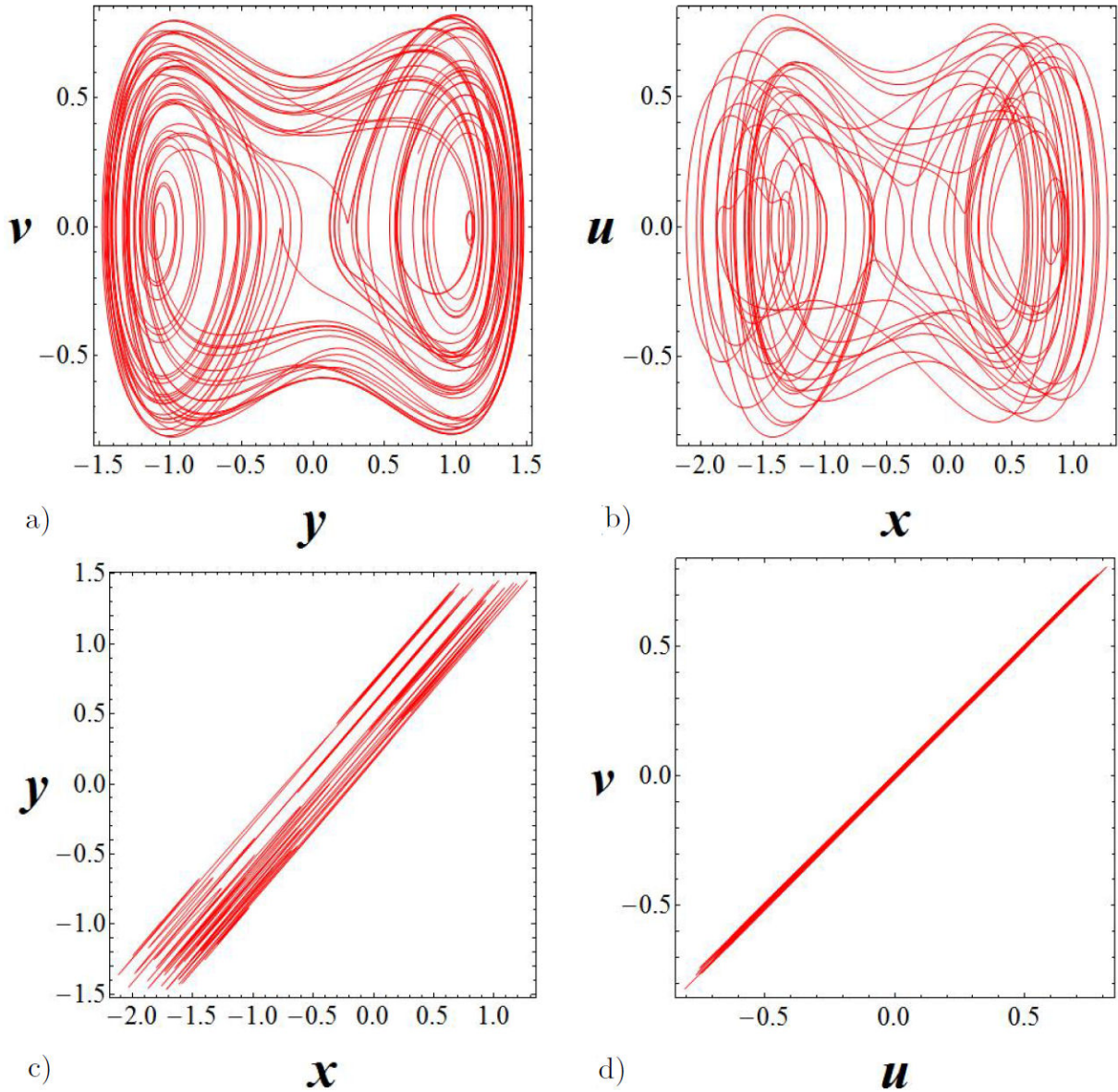
FIGURE 8. Dissipative coupling case, for $H = 200$. In a) The Duffing oscillator (master) and in b) the van der Pol oscillator (slave). In c) and d) the phase space for the $y - x$ and $v - u$ channels respectively.

In particular, in Ref. [24] a modified master-slave scheme is considered that leads to synchronization even in the cases where the classical master-slave scheme fails. The approach used in Ref. [24] uses a non conventional coupling, where a linear feedback occurs. The coupling can be seen as a perturbation to each oscillator proportional to the difference of the position (elastic coupling), $G(y - x)$, which is introduced in the velocity of the slave system. The coupling also uses another linear feedback, that can be seen as perturbation to each oscillator proportional to the difference of the velocity (dissipative coupling), $G(v - u)$, introduced in the acceleration in the slave system. For the van der Pol-Duffing system, the equations read as

Master: $\begin{cases} \dot{y} = v, \\ \dot{v} = -\alpha v + y - \varepsilon y^3 + A_1 \cos(\omega_1 t), \end{cases}$ (18)

Slave: $\begin{cases} \dot{x} = u + G(y - x), \\ \dot{u} = \mu(1 - x^2)u - x + A_2 \cos(\omega_2 t) + G(v - u). \end{cases}$ (19)

Notice, again, that for $G = 0$, the equations decouple. In order to get more insight in the physical meaning of this case, let us assume that $G \gg \mu$. Thus, Eq. (19) can be cast as

$$\ddot{x} + 2G\dot{x} + (1 + G^2)x = A_2 \cos(\omega_2 t) + 2G\dot{y} + G^2 y. \quad (20)$$
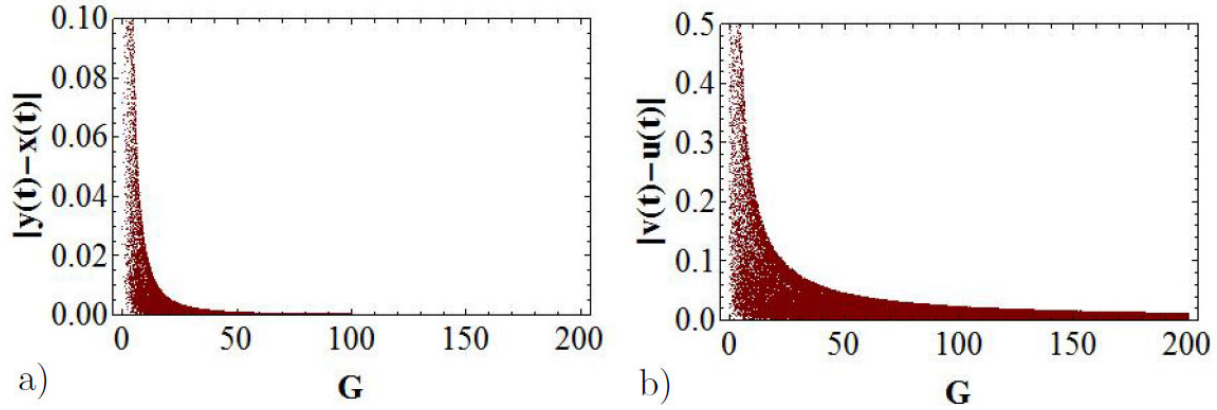
FIGURE 9. Bifurcation diagrams for the error functions. In a) it is represented $\mid y(t) - x(t) \mid$, and in b) $\mid v(t) - u(t) \mid$, both as a function of the parameter G.
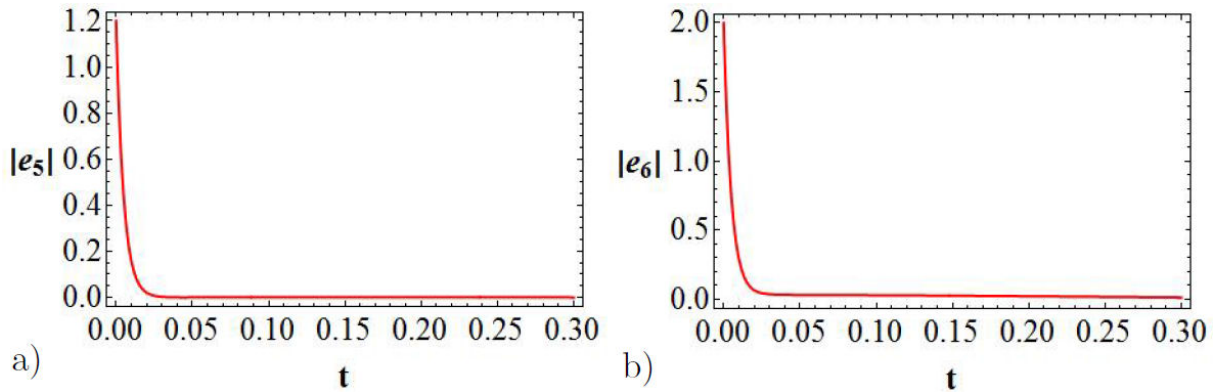

FIGURE 10. Error functions $|e_5|$ and $|e_6|$ for $G = 200$.

The left hand side of the equation depends only on the x while the right hand side depends only on y, except for the external harmonic forcing. Thus, the oscillators synchronize in both channels $y - x$ and $v - u$. In the last case, we have

$$\dot{v} - \dot{u} - G(v - u) - G^2(y - x) = \ddot{y} - \ddot{x} \approx 0, \qquad (21)$$

that is, if there is synchronization in the $y - x$ channel (both oscillators follow the same dynamics) then in the $v - u$ channel there is also synchronization. We should emphasize that, by comparing with the former cases, in the dissipative coupling only was possible to reach synchronization in the $v - u$ channel, and in the elastic coupling no synchonization exists.

We study the dynamics of the system varying the coupling constant G. In order to analyze the bifurcation diagrams, let us consider the error functions $\mid y(t) - x(t) \mid$ and $\mid v(t) - u(t) \mid$, by varying G from 0 to 200. The error functions allow us to find the range of G for which the synchronization is produced in the $y-x$ and $v-u$ channels. As it can be observed in Figs. 9a) and b), we obtain total synchronization in the $y - x$ and $v - u$ channels, since the error function tends to zero as the value of G is increased. For the coupling proposed in Ref. [24], that combines elastic and dissipative couplings, the errors $e_5 = y - x$ and $e_6 = v - u$ are obtained

by taking the difference of Eqs. (18) and (19), giving

$$\dot{e}_5 = \dot{y} - \dot{x} = v - u - Ge_5,$$

$$e_6 = v - u = \dot{e}_5 + Ge_5,$$

$$\dot{e}_6 = -\alpha v + y - \varepsilon y^3 + A_1 \cos(\omega_1 t)$$
$$- \mu(1 - x^2)u + x - A_2 \cos(\omega_2 t) - G(e_6). \qquad (22)$$

The plots of $|e_5|$ and $|e_6|$ as a function of t, for a value of $G = 200$, are depicted in Fig. 10.

Let us now analyze the phase space for the $y-x$ and $v-u$ channels for the value $G = 200$. In Figs. 11c) and d) it can be observed that total synchronization is reached since the error function in the phase space is represented by a straight line at $45°$ in both channels.

By comparing the three different coupling above mentioned, we observed that the coupling used by Uriostegui *et al.* gives the best results. In fact, by using the former coupling, we observed that total synchronization in both $y - x$ and $v - u$ channels is achieved.

In order to analyze the case of two different values in the couplings its is convenient, for our discussion, to express the couplings in terms of the errors: for the elastic coupling we have $G(y - x) = G(e_5)$, whilst for the dissipative coupling
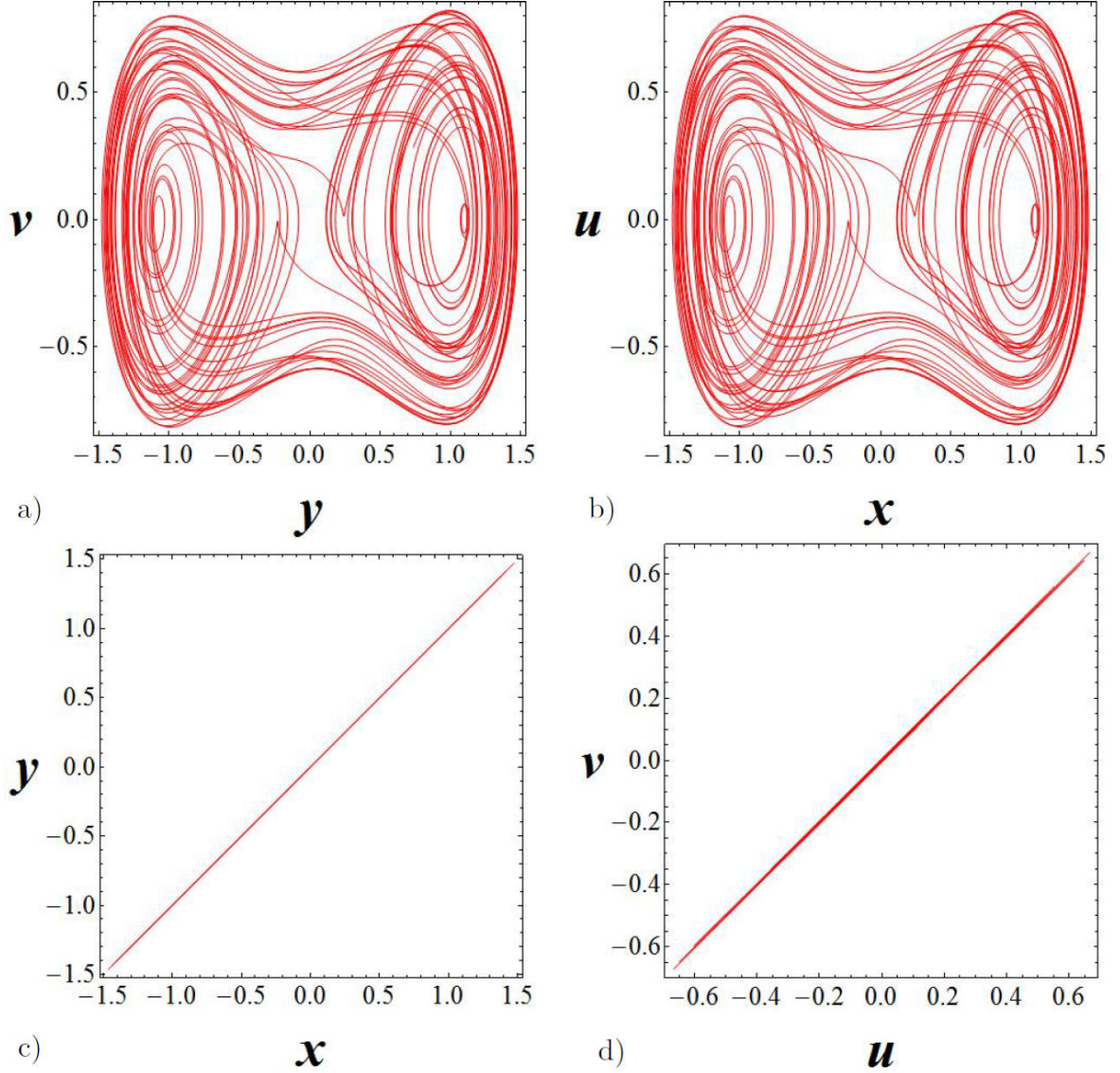
FIGURE 11. Elastic and dissipative couplings for $G = 200$. In a) the Duffing oscillator (master). In b) the van der Pol oscillator (slave). In c) and d) the phase space for the $y - x$ and $v - u$ channels.

$G(v - u) = G(\dot{e}_5 + Ge_5)$. In Figs. 9a) and b), we can appreciate that synchronization in the $y - x$ channel is obtained for values of G smaller than those in the $v - u$ channel. Let us now analyze the case of two different constants G_1 and G_2. For this, the evolution of the system is governed by

$$\text{Master} : \begin{cases} \dot{y} = v, \\ \dot{v} = -\alpha v + y - \varepsilon y^3 + A_1 \cos(\omega_1 t), \end{cases} \quad (23)$$

$$\text{Slave} : \begin{cases} \dot{x} = u + G_1(y - x), \\ \dot{u} = \mu(1 - x^2)u - x + A_2 \cos(\omega_2 t) + G_2(v - u). \end{cases} \quad (24)$$

As before, let us assume that $G_2 \gg \mu$. In this case, Eq. (24)

reduces to

$$\ddot{x} + (G_1 + G_2)\dot{x} + (1 + G_1 G_2)x = A_2 \cos(\omega_2 t)$$
$$+ (G_1 + G_2)\dot{y} + G_1 G_2 y.$$

Once again, by comparing with Eq. (20), we observe that, to obtain synchronization, we must assume $G_2 \approx G_1$ or $G_2 \gg G_1$. In what follows we analyze the last case.

The errors $e_7 = y - x$ and $e_8 = v - u$, are determined by subtracting Eqs. (23) and (24), obtaining

$$\dot{e}_7 = \dot{y} - \dot{x} = v - u - G_1 e_7,$$

$$e_8 = v - u = \dot{e}_7 + G_1 e_7,$$

$$\dot{e}_8 = -\alpha v + y - \varepsilon y^3 + A_1 \cos(\omega_1 t)$$
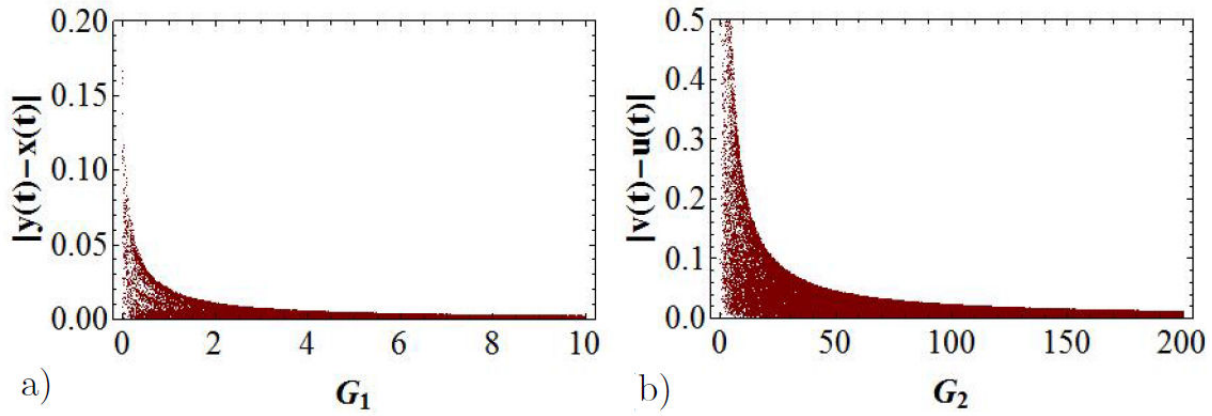$$- \mu(1 - x^2)u + x - A_2 \cos(\omega_2 t) - G_2(e_8). \quad (25)$$

FIGURE 12. Bifurcation diagrams for the error functions. In (a) it is represented $\mid y(t) - x(t) \mid$, with $G_2 = 100$ and varying G_1. In (b) $\mid v(t) - u(t) \mid$, with $G_1 = 10$ and varying G_2.
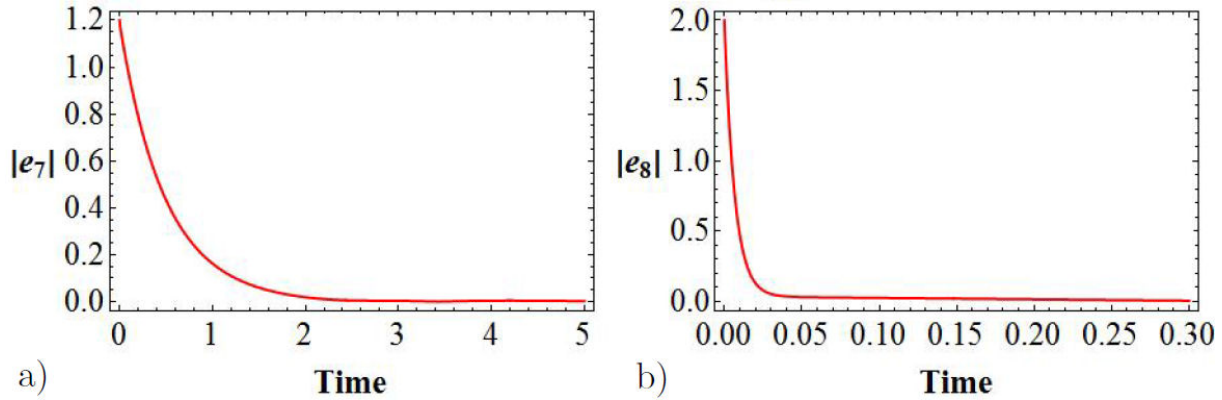

FIGURE 13. Error functions for $|e_7|$ and $|e_8|$ with respective values of $G_1 = 2$ and $G_2 = 150$.

The constant G_1 corresponds to the elastic coupling and G_2, to the dissipative coupling. Hence, $G_1(y - x) = G_1(e_7)$ and $G_2(v - u) = G_2(\dot{e}_7 + G_1 e_7)$. Let us express Eqs. (23) and (24) in a matrix form

$$\begin{pmatrix} \dot{y} \\ \dot{v} \end{pmatrix} = \begin{pmatrix} 0 & 1 \\ 1 & -\alpha \end{pmatrix} \begin{pmatrix} y \\ v \end{pmatrix}$$
$$+ \begin{pmatrix} 0 \\ -\varepsilon y^3 \end{pmatrix} + \begin{pmatrix} 0 \\ A_1 \cos(\omega_1 t) \end{pmatrix}, \qquad (26)$$

$$\begin{pmatrix} \dot{x} \\ \dot{u} \end{pmatrix} = \begin{pmatrix} 0 & 1 \\ -1 & \mu \end{pmatrix} \begin{pmatrix} x \\ u \end{pmatrix}$$
$$+ \begin{pmatrix} 0 \\ -\mu x^2 u \end{pmatrix} + \begin{pmatrix} 0 \\ A_2 \cos(\omega_2 t) \end{pmatrix}$$
$$+ \begin{pmatrix} G_1 e_7 \\ G_2 \dot{e}_7 + G_1 G_2 e_7 \end{pmatrix}. \qquad (27)$$

The first vectors in the right hand side of Eqs. (26) and (27) contain the nonlinearity information of the system, while the second ones contain the information of the external forcing. The last vector in Eq. (27) is the so-called control vector,

which contains the coupling we propose. Notice that the control depends on the error and its derivative. For the case $G_1 = G_2 = 0$ de system decouples. In order to study the dynamics of the system, we vary the couplings G_1 or G_2 keeping one constant. To analyze the bifurcation diagrams, let us consider the error functions $\mid y(t) - x(t) \mid$ and $\mid v(t) - u(t) \mid$. We calculate $\mid y(t) - x(t) \mid$ keeping $G_2 = 100$ and varying G_1 from 0 to 10. In a similar way, we obtain the bifurcation diagram for the error function $\mid v(t) - u(t) \mid$ with $G_1 = 10$ and varying G_2 from 0 to 200. As it can be appreciated in Figs. 12a) and b), we obtain total synchronization in the $y - x$ and $v - u$ channels, since the error functions go to zero as the values of G_1 and G_2 are increased. The plots of $|e_7|$ and $|e_8|$ as a function of t, for the values of $G_1 = 2$ and $G_2 = 150$, are depicted in Fig. 13.

Let us now analyze the phase space for the $y - x$ and $v - u$ channels, for values of $G_1 = 2$ and $G_2 = 150$. In Figs. 14c) and d), we can observe that total synchronization is reached, since the error functions in the phase space is represented by a straight line at $45°$ in both channels.
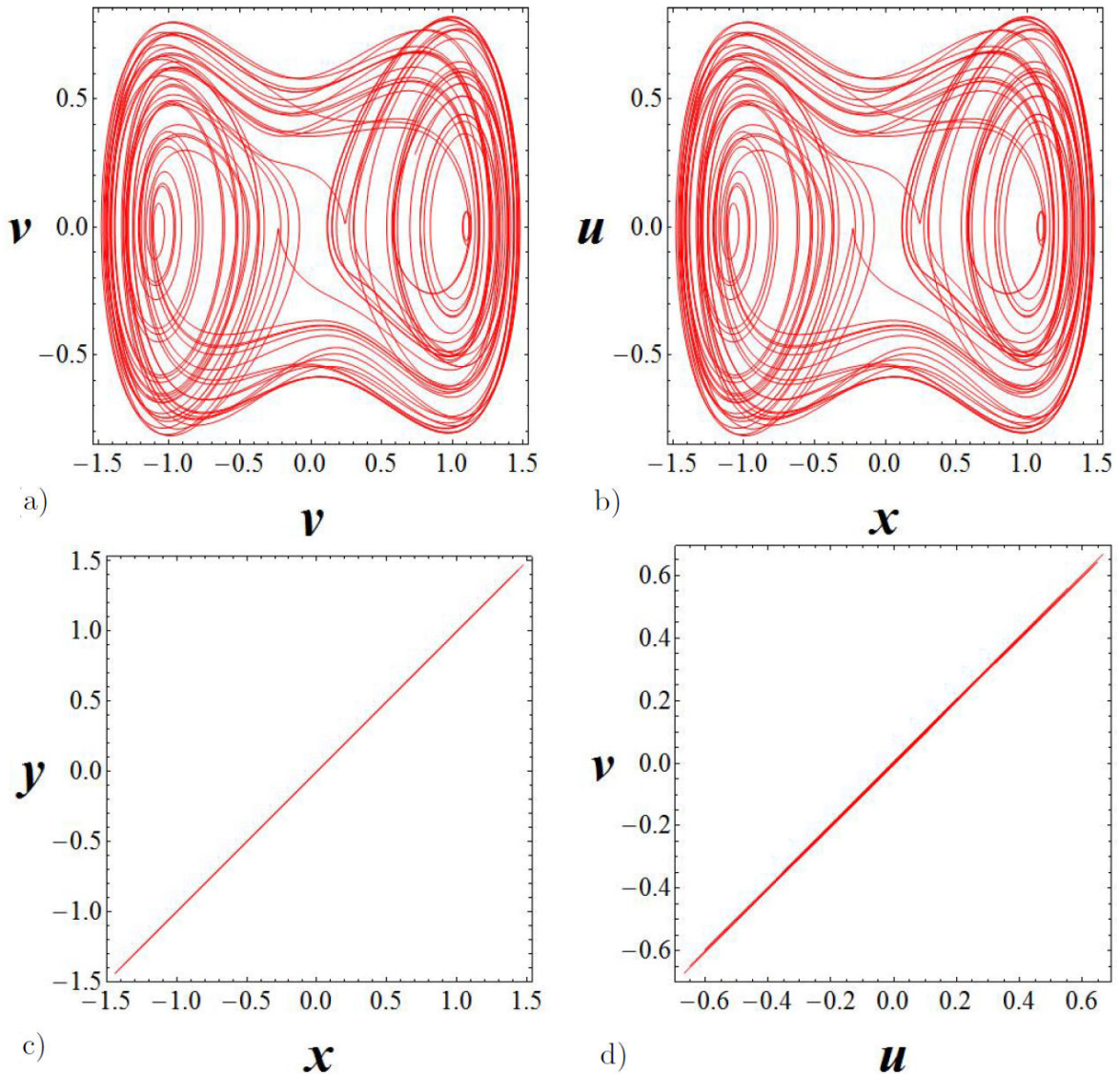
FIGURE 14. Elastic and dissipative couplings for $G_1 = 2$ and $G_2 = 150$. In a) the Duffing oscillator (master). In b) the van der Pol oscillator (slave). In c) and d) the phase space for $y - x$ and $v - u$ channels.

4. Final remarks and outlook

The van der Pol and Duffing are nonautonomous systems of low-dimensionality that present chaos and have been well studied. One of the conclusions presented in the literature related to these systems is that the elastic coupling does not lead to synchronization. For this same system, when the dissipative coupling is used, only synchronization in one channel can be obtained. In this paper, we have analyzed the synchronization in the van der Pol-Duffing system based on two different couplings simultaneously employed, namely the elastic and dissipative. We used the error function by varying the control parameters, K, H, G or G_1 and G_2 (depending on the coupling used), which enabled us to obtain the range for which the synchronization takes place. We found that the synchronization was favored for rather large values of the control parameter.

We also observed that, the coupling that blend the elastic and dissipative, leds to total synchronization in the $y - x$ and $v - u$ channels. In this case the synchronization was obtained for values of G large enough (in our numerical simulations, we took $G = 200$). For small values, we obtained partial synchronization. For the general case, when two constants coupling are used, G_1 (elastic) and G_2 (dissipative), with $G_1 \ll G_2$, we get again synchronization in both channels. Whether G_2 is small and comparable with G_1 the system presents partial synchronization in the $v - u$ channel and total synchronization in the $y - x$ channel. The behavior of the system in the mentioned cases were explained analytically and numerically corroborated, for the case large values of the parameters.

The possibility of using two coupling constant instead of only one, allows the system a more interesting dynamics and

a broad range for the control parameters. It is well known that synchronization in communication systems needs a large range for the control parameter, such as the obtained, for the van Pol-Duffing system, by employing our approach of coupling. Consequently, the system studied could be of usefulness in this communication systems. The coupling studied in this work will be applied in others systems of low-dimensionality that do not present synchronization through the classical master-slave configuration.

Acknowledgements

1. L.M. Pecora and T.L. Carroll, Synchronization in chaotic systems, *Phys. Rev. Lett.* **64** (1990) 821, https://doi.org/10.1103/PhysRevLett.64.821.

2. I. Pastor-Diaz and A. López-Fraguas, Dynamics of two coupled van der Pol oscillators, *Phys. Rev. E* **52** (1995) 1480. https://doi.org/10.1103/PhysRevE.52.1480.

3. C. Reick and E. Mosekilde, Emergence of quasiperiodicity in symmetrically coupled, identical period-doubling systems, *Phys. Rev. E* **52** (1995) 1418, https://doi.org/10.1103/PhysRevE.52.1418.

4. M. Z. Ding and W. H. Yang, and H. J. Zhang, Observation of intermingled basins in coupled oscillators exhibiting synchronized chaos *Phys. Rev. E* **54** (1995) 2489. https://doi.org/10.1103/PhysRevE.54.2489.

5. H-W. Yin and J-H. Dai, Phase effect of two coupled periodically driven Duffing oscillators, *Phys. Rev. E* **58** (1998) 5683, https://doi.org/10.1103/PhysRevE.58.5683.

6. K-J. Lee, Y. Kwak and T-K. Lim, Phase jumps near a phase synchronization transition in systems of two coupled chaotic oscillators, *Phys. Rev. Lett.* **81** (1998) 321. https://doi.org/10.1103/PhysRevLett.81.321.

7. L.O. Chua, M. Itoh, L. Kocarev and K. Eckert, Chaos synchronization in Chua's circuit, *J. Circuits Syst. Comput.* **3** (1993) 93, https://doi.org/10.1142/S0218126693000071.

8. A.P. Kuznetsov, and J.P. Roman, Properties of synchronization in the systems of non-identical coupled van der Pol and van der Pol-Duffing oscillators. Broadband synchronization, *Phys. D* **238** (2009) 1499. https://doi.org/10.1016/j.physd.2009.04.016.

9. M. G. Rosenblum, A. Pikovsky and J. Kurths, From phase to lag synchronization in coupled chaotic oscillators, *Phys. Rev. Lett.* **78** (1997) 4193. https://doi.org/10.1103/PhysRevLett.78.4193.

10. K. Murali and M. Lakshmanan, Transmission of signals by synchronization in a chaotic Van der Pol-Duffing oscillator, *Phys. Rev. E* **48** (1993) R1624, https://doi.org/10.1103/PhysRevE.48.R1624.

11. A.N. Njah, Synchronization via active control of parametrically and externally excited Φ^6 Van der Pol and Duffing oscillators and application to secure communications, *J. Vib. Control* **17** (2010) 504, https://doi.org/10.1177/1077546309357024.

12. L. Lu, F. Zhang and C. Han, Synchronization transmission of the target signal in the circuit network based on coupling technique, *Physica A: Statistical Mechanics and its Applications* **535** (2019) 122412, https://doi.org/10.1016/j.physa.2019.122412.

13. M. S. Dutra, A.C. de Pina Filho and V.F. Romano, Modeling of a bipedal locomotor using coupled nonlinear oscillators of Van der Pol, *Biol. Cybern.* **88** (2003) 292, https://doi.org/10.1007/s00422-002-0380-8.

14. F. Jasni and A. A. Shafie, Van Der Pol Central Pattern Generator (VDPCPG) Model for Quadruped Robot, in Intelligent Robotics, Automation, and Manufacturing (Springer, Berlin, 2012), Vol. 330, p. 175, https://doi.org/10.1007/978-3-642-35197-6_18.

15. S. Mall and S. Chakraverty, Hermite Functional Link Neural Network for Solving the Van der Pol-Duffing Oscillator Equation, *Neural Comput.* **28** (2016) 1598, https://doi.org/10.1162/NECO_a_00858.

16. S. S. Chaharborj, S. S. Chaharborj, and P. P. See, Application of Chebyshev neural network to solve Van der Pol equations, *Int. J. Basic Appl. Sci. 10* (2021) 7, https://www.sciencepubco.com/index.php/ijbas/article/view/31431.

17. D. Pazó and E. Montbrió, Low-dimensional dynamics of populations of pulse-coupled, *Phys. Rev. X* **4** (2014) 011009, https://doi.org/10.1103/PhysRevX.4.011009.

18. M. Zhang, G.S. Wiederhecker, S. Manipatruni, A. Barnard, P. McEuen, and M. Lipson, Synchronization of micromechanical oscillators using light, *Phys. Rev.* **109** (2012) 233906. https://doi.org/10.1103/PhysRevLett.109.233906.

19. J.C. Chedjou, K. Kyamakya, I. Moussa, H.P. Kuchenbecker, and W. Mathis, Behavior of a self sustained electromechanical transducer and routes to chaos, *J. Vib. Acoust.* **128** (2006) 282. https://doi.org/10.1115/1.2172255.

20. J.C. Chedjou, H.B. Fotsin, P. Woafo, and S. Domngang, Analog simulation of the dynamics of a van der Pol oscillator coupled to a Duffing oscillator, IEEE Trans. Circuits Syst. I, *Fundam. Theory Appl.* **48** (2001) 748. https://doi.org/10.1109/81.928157.

21. A.P. Kuznetsov, N.V. Stankevich, and L.V. Turukina, Coupled van der Pol-Duffing oscillators: phase dynamics and structure of synchronization tongues, *Physica D* **238** (2009) 1203. https://doi.org/10.1016/j.physd.2009.04.001.

22. M.S. Siewe, S.B. Yamgoué, E.M. Moukam Kakmeni and C. Tchawoua, Chaos controlling self-sustained electromechanical seismograph system based on the Melnikov theory, *Nonlinear Dyn.* **62** (2010) 379. https://doi.org/10.1007/s11071-010-9725-3.

23. U.E. Vincent, A. Kenfack, Synchronization and bifurcation structures in coupled periodically forced non-identical Duffing oscillator, *Phys. Scr.* **77** (2008) 045005. `https://doi.org/10.1088/0031-8949/77/04/045005`.

24. U. Uriostegui, E.S. Tututi and G. Arroyo, A new scheme of coupling and synchronizing low-dimensional dynamical systems, *Rev. Mex. Fis.* **67** (2021) 334. `https::https://doi.org/10.31349/RevMexFis.67.334`.

25. J. Kengne, J.C. Chedjou, G. Kenne, K. Kyamakya, and G.H. Kom, Analog circuit implementation and synchronization of a system consisting of a van der Pol oscillator linearly coupled to a Duffing oscillator, *Nonlinear Dyn*, **70** (2012) 2163. `https://doi.org/10.1007/s11071-012-0607-8`.

26. J. Kengne, F. Kenmogne, and V. Kamdoum Tamba, Experiment on bifurcation and chaos in coupled anisochronous self-excited systems: Case of two coupled van der Pol-Duffing oscillators, *Journal of Nonlinear Dynamics* **2014** (2014) 815783. `https://doi.org/10.1155/2014/815783`.

27. H. Zhang, D. Liu and Z. Wang, *Controlling Chaos: Suppression, Synchronization and Chaotification*, Springer, London, (2009). `https://doi.org/10.1007/978-1-84882-523-9`.

28. S. Boccaletti, J. Kurths, G. Osipov, DL. Valladares and CS. Zhou, The synchronization of chaotic systems, *Physics Reports* **366** (2002) 101. `https://doi.org/10.1016/S0370-1573(02)00137-0`.

29. L. M. Pecora and T. L. Carroll Synchronization of chaotic systems, *Chaos*, **25** (2015) 097611. `https://doi.org/10.1063/1.4917383`.

30. L. Thomas and L. M. Pecora, Synchronizing nonautonomous chaotic circuits, *IEEE Trans. on Circuits and Systems-II*, **40** (1993) 646, `https://doi.org/10.1109/82.246166`.

31. W-C C. Chan and Y-D Chao, Synchronization of coupled forced oscillators, *J. Math. An. and Applications* **218** (1998) 97, `https://doi.org/10.1006/jmaa.1997.5749`.

32. T-P Chang, Chaotic motion in forced duffing system subject to linear and nonlinear damping, *Mathematical Problems in Engineering*, **2017** (2017) 3769870. `https://doi.org/10.1155/2017/3769870`.

33. M. S. Siewe, C. Tchawoua, and P. Woafo, Melnikov chaos in a periodically driven Rayleigh-Duffing oscillator, *Mechanics Research Communications*, **37** (2010) 363, `https://doi.org/10.1016/j.mechrescom.2010.04.001`.

34. Y-Z. Wang, and F-M. Li, Dynamical properties of Duffing-van der Pol oscillator subject to both external and parametric excitations with time delayed feedback control, *J. Vibration and Control* **21** (2015) 371, `https://doi.org/10.1177/1077546313483160`.

35. K. Ding, Master-Slave Synchronization of Chaotic Φ^6 Duffing Oscillators by Linear State Error Feedback Control, *Complexity* **2019** (2019) 3637902, `https://doi.org/10.1155/2019/3637902`.

36. A. Buscarino, L. Fortuna, and L. Patane, *Master-slave synchronization of hyperchaotic systems through a linear dynamic coupling*, *Phys. Rev. E* **100** (2019) 032215, `https://doi.org/10.1103/PhysRevE.100.032215`.

37. F. Aydogmus and E. Tosyali, Master-slave synchronization in a 4D dissipative nonlinear fermionic system, *International Journal of Control* **2020** (2020) 1, `https://doi.org/10.1080/00207179.2020.1808244`.

38. J.P. Ramirez, E. Garcia and J. Alvarez, Master-slave synchronization via dynamic control, *Commun Nonlinear Sci Numer Simulat*, **80** (2020) 104977. `https://doi.org/10.1016/j.cnsns.2019.104977`.